ORIGINAL ARTICLE

A quantitative approach for measuring crowding in the dental arch: Fourier descriptors

Pete E. Lestrel, PhD,[a] Osamu Takahashi, DDS, PhD,[b] and Eisaku Kanazawa, PhD[c]
Van Nuys, Calif, and Matsudo and Tokyo, Japan

Dental crowding is defined as a discrepancy between tooth size and jaw size that results in a misalignment of the tooth row. Proposed reasons for crowding include excessively large teeth, small jaws, and a combination of both. Nevertheless, the parameters that would allow the prediction of crowding have not been identified. This study compared the shape of crowded and uncrowded dental arches, matched for size and sex. The application of elliptical Fourier functions (EFFs) provided an accurate numeric description of the dental arch form. Dental casts from the Nihon University School of Dentistry at Matsudo, Chiba, Japan, were studied. Group I, the control group, consisted of 118 dental cast pairs (49 female, 69 male, aged 20.40 ± 1.68 years [mean ± SD]) with little or no crowding. Group II, which exhibited crowding, consisted of 78 dental cast pairs (64 female, 14 male, aged 19.67 ± 4.95 years). From photographs, a set of 24 homologous points describing the tooth row was identified. These points were then fitted with EFFs. Each maxillary and mandibular outline was subsequently standardized for size by scaling the bounded area to a constant 10,000 mm^2. These "shape only" data were used to assess differences between arches in the 2 groups. By multivariate analysis of variance, statistically significant shape differences between groups I and II were obtained for both arches. Patients with crowding exhibited more variability than did the controls. This variability was illustrated with canonical axes derived from discriminant function analysis. (Am J Orthod Dentofacial Orthop 2004;125:716-25)

The prevalence of crowding in the dental arch is increasing in the modern Japanese dentition. One consequence of this has been an increase in malocclusions because of discrepancies between jaw size and dental arch size.[1,2] Reasons for this increase in crowding are complex, and various explanations have been offered.[3,4] These include changes in dietary habits leading to a reduction in masticatory function, reduced mechanical stresses, actual increases in tooth size, and absence of proximal wear. Whatever the causes, it is apparent that an outcome of this dental-arch-size-to-jaw-size discrepancy is crowding.

A quantitative assessment of crowding has not been easily attainable. Crowding exhibits extensive irregularities along the anterior aspect of the dental arch that are difficult to describe numerically with distances and angles. Thus, more sophisticated numeric methods are required. Leaving crowding aside for the moment, various procedures, both qualitative and quantitative, have been proposed to describe the form of the normal dental arch. Early attempts were largely in terms of qualitative descriptions, such as "parabolic," "elliptical," and "U-shaped," which tend to be typologic and unsatisfactory. This prompted a search for more sophisticated mathematic methods. Most of these curve-fitting approaches include conic sections like parabolas and ellipses, the catenary curve, cubic splines, and regular and orthogonal polynomials.[5]

One of the earliest attempts to describe the form of the normal dental arch is the work of MacConail et al,[6] who fitted a catenary curve. A catenary curve can be estimated with a free-hanging chain supported at the ends.[7] Conic sections, such as the parabola, were also applied by various authors.[8-11] BeGole[12] fitted cubic spline curves. An early study by Lu[13] applied orthogonal polynomials. Mixed models, which use 2 functions, 1 for the anterior and 1 for the posterior dentition, have also been applied.[14]

Because most of those models have been tested on normal subjects (those with little or no crowding), their application to patients with crowding is limited. Yet, it is exactly those patients who are of special interest to orthodontists, prosthodontists, and oral surgeons. Most

[a]Professor emeritus, Sections of Orthodontics and Oral Biology, University of California-Los Angeles School of Dentistry.
[b]Private practice, Tokyo, Japan; formerly of the Department of Orthodontics, Nihon University School of Dentistry at Matsudo, Japan.
[c]Department of Anatomy, Nihon University, School of Dentistry at Matsudo.
Reprint requests to: Pete E. Lestrel, 7327 De Celis Pl, Van Nuys, CA 91406-2853; e-mail, plestrel@earthlink.net.
Submitted, April 2003; revised and accepted, May 2003.
0889-5406/$30.00

doi:10.1016/j.ajodo.2003.05.008

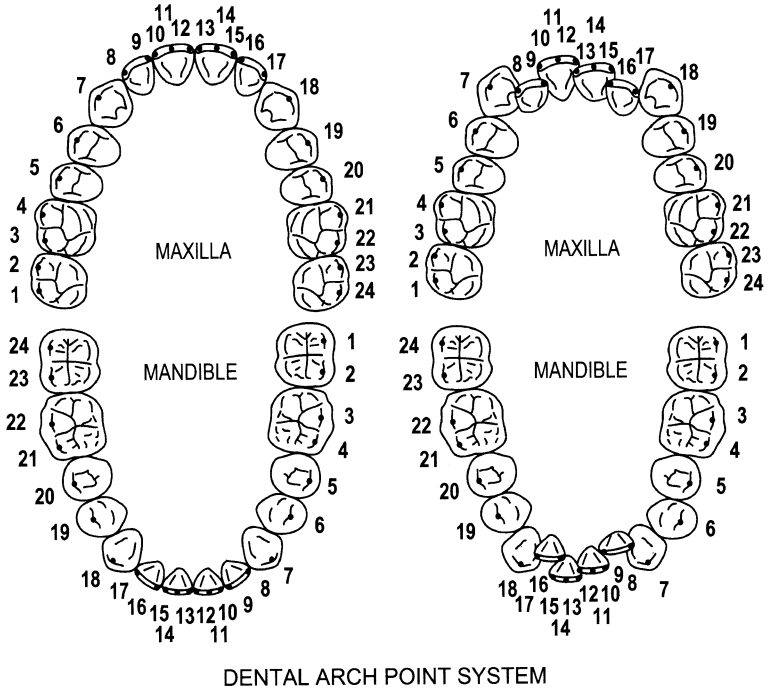

Fig 1. MX and MD arches, with control case (good occlusion) on left and crowding case on right. *Black dots* depict 24 points used to describe 2 arch forms.

of these models suffer from 2 deficiencies: (1) they generally do not separate the influence of size from that of shape, and (2) they are difficult to apply to cases of crowding. Consequently, a morphometric method that addresses these issues is required.

A particular Fourier descriptor, elliptical Fourier functions (EFFs), increasingly has been used to numerically describe the boundary outline of irregular 2-dimensional morphologies. This algorithm was developed by Kuhl and Giardina[15] and has now been successfully applied in rather diverse disciplines, including pattern recognition engineering, geology, paleontology, biology, dentistry, and medicine.[16-22] EFFs are particularly attractive for characterizing complex irregular forms of the type encountered in the craniofacial complex. The purpose of this study was 4-fold: (1) to assess the fit of EFFs to the dental arch, (2) to detect differences in shape, (3) to explore sexual dimorphism in shape, and (4) to compare normal with crowded dentitions.

MATERIAL AND METHODS

Dental casts of 112 female and 83 male subjects were available from the Nihon University Dental School at Matsudo, Chiba Prefecture. These 195 subjects represented 2 groups: (1) healthy Japanese dental students, aged 18 to 25 years; and (2) patients from the Nihon University Dental Hospital at Matsudo, aged 12 to 33 years. Criteria for inclusion in the sample were as follows: (1) no current or previous orthodontic treatment, (2) no symptoms of temporomandibular dysfunction, (3) no bridges or other restorations, (4) minimal attrition, and (5) all permanent teeth present (except third molars).

Maxillary (MX) and mandibular (MD) dental casts were analyzed separately for the 2 samples. These samples were then subdivided into 2 groups; group I ($n = 118$; aged 20.40 ± 1.68 years [mean $\pm$ SD]) included clinically normal dental cast pairs (those with minimal or no crowding); group II ($n = 77$; aged 19.67 ± 4.95 years) consisted of dental cast pairs with crowding in at least 1 arch. The groups were further divided by sex; group I (controls) consisted of 49 female and 69 male subjects. Group II (crowding) consisted of 60 female and 14 male subjects for the MX dentition, and 63 female and 14 male subjects for the MD dentition. The discrepancy in numbers between the MX and MD dentitions was due to missing casts from the available database.

The MX and MD dental models were photographed separately, each with a ruler to ensure careful control of magnification. Negative 35-mm (24×36 mm) film (Neopan SS ISO 100/21°, Fuji Photo Film, Tokyo, Japan) was used with a Nikon FM2 camera (Nikon,

Tokyo, Japan) fitted with a 105-mm Micro-Nikkor lens (Nikon) to minimize distortion. The photographic technique was standardized. The occlusal plane was determined by connecting the right and left mesiobuccal cusps of the first molars and the incisal edge of the left central incisor. If the left central incisor was out of place, the right central incisor was used. The film plane was placed parallel to the occlusal plane at a constant distance of 600 mm. To ensure that the photographs were the same size as the original specimens, standardized (1:1) prints were then made with Fuji black-and-white paper (WPFM3; Fuji Photo Film).

Twenty-four landmarks, describing the right and left tooth rows from the central incisor to the second molar, were carefully marked on the photographs with a fine pen (Fig 1). These 24 landmarks were then directly digitized (DrawingBoard III; Calcomp, Scottsdale, Ariz) and submitted to a specially written program, EFF23, which first generated an intermediate file. This new intermediate file used the above digitized data and created a "mirror-image" about a line connecting the right and left distal cusps of the second molars. This can also be viewed as a reflection about the x-axis (Fig 2). A consequence of this reflection is a doubling of the number of observed points to 48. This configuration, which is now symmetric with respect to the x-axis, has mathematic advantages to be discussed below.

The procedure of using EFFs represents a parametric solution. That is, the representation of the x and y points on a curve in 2 dimensions is in the form of a pair of equations as functions of a third variable *(t)*. Any 2-dimensional outline can be approximated with a polygon by connecting the observed data points with straight lines. The parametric equations that define the EFF are such that the Fourier series in *x(t)* is given as:

$$x(t) = A_0 + \sum_{n=1}^{k} a_n \cos(nt) + \sum_{n=1}^{k} b_n \sin(nt)$$

and the Fourier series in *y(t)* as:

$$y(t) = C_0 + \sum_{n=1}^{k} c_n \cos(nt) + \sum_{n=1}^{k} d_n \sin(nt)$$

where n equals the harmonic number, k equals the maximum harmonic number, and the interval is over 2π. The 4 coefficients, a_n, b_n, c_n, and d_n, as well as the 2 constants, A_0 and C_0, must be estimated. Thus, 24 harmonics require the computation of 98 series terms. Details regarding the EFF formulation can be found in Kuhl and Giardina[15] and Lestrel.[21] (For those interested, the EFF23 program is available from the first author).

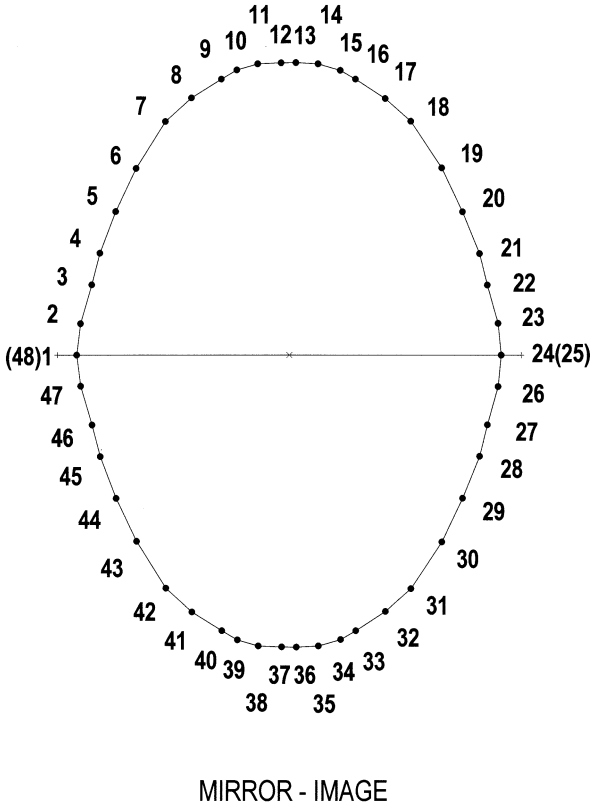

Fig 2. To bound dental arch form, 24 original points on each MX and MD arch were digitized. Then, computer-generated "mirror image" was created as reflection about x-axis. This led to doubling of observed points to 48. This configuration is now symmetric about x-axis.

EFFs were calculated for each MX and MD dental cast. The 48 points were doubled again, to 96, to generate smoother EFF curves. That these EFFs are close analogues of the now-bounded MX and MD outlines can be determined from the residual or difference between the observed points and the predicted points (expected fit) from the Fourier function. The use of 24 harmonics (the number of harmonics is limited to half the number of points because of Nyquist frequency constraints) yielded a residual of 0.24 ± 0.05 mm ($n = 76$), which is less than the point location and digitizing errors.

There is an approximately 5% sexual dimorphism in size in human skeletal bones, with females being smaller.[23] This sexual dimorphism is also present in the dental arches and can play a confounding role in analysis. Consequently, a procedure was instituted to standardize each dental cast for size. Size-standardization was accomplished by scaling all bounded dental cast outlines to a constant area of 10,000 mm^2.

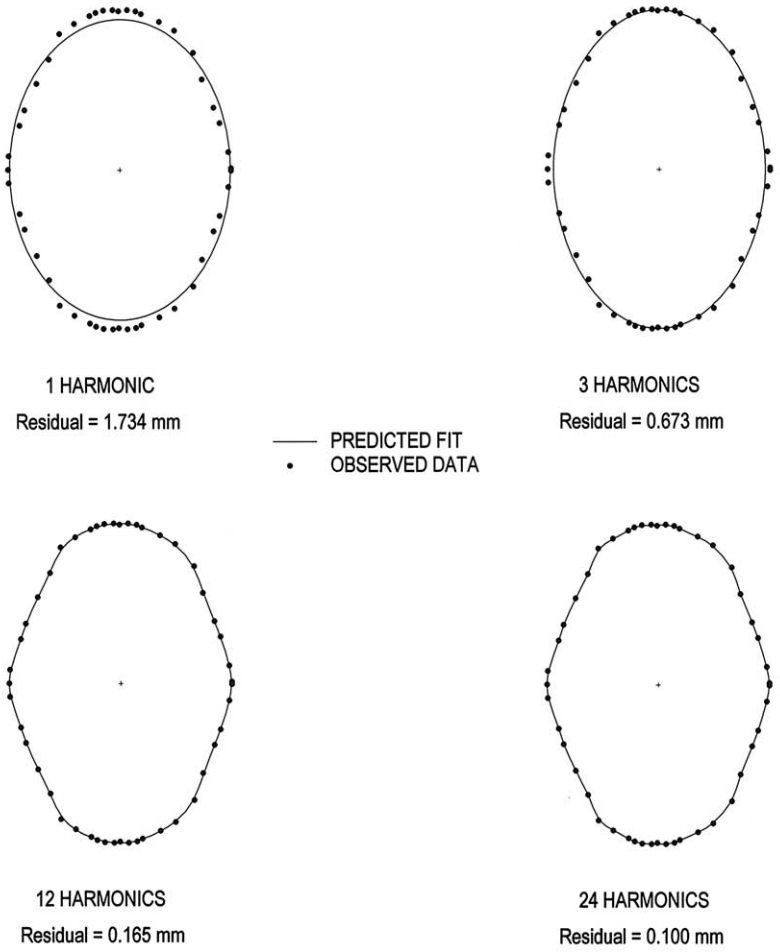

Fig 3. Computer-generated 2-dimensional lateral view of control MD outline that has been reflected. *Dots* represent observed 48 digitized points. Elliptical Fourier function is shown here as stepwise process to demonstrate convergence of Fourier series. First harmonic represents ellipse. With addition of 3 harmonics, mean residual fit between expected function and observed data points was 0.67 mm overall. With 24 harmonics, mean residual dropped to 0.10 mm.

The convergence of the EFF and the closeness of the final curve-fit to the observed dental cast outline are illustrated as a stepwise process in Figure 3. Because the dental cast outline is already rather elliptical, the first harmonic will have a large contribution. Thus, with 1 harmonic, the mean residual for this case is already small, 1.73 mm. With 3 harmonics, the residual reduces to 0.67 mm; with 12 harmonics, it is 0.17 mm; and with 24 harmonics, this value drops to 0.10 mm.

With EFFs, 2 distance data sets were constructed. One distance data set was composed of distances from the centroid to the dental cast outline, and the other represented individual or point-to-point distances (Fig 4). The choice of distances, instead of the more commonly used amplitudes, was based on 2 considerations: (1) the need for localized measures, which amplitudes do not provide, and (2) difficulties in interpreting what the amplitudes are measuring in a biological context.[21,22]

Statistical procedures

The statistical design consisted of testing for statistically significant differences in sex (female versus male) and type (crowding versus controls). With the standardized-for-size EFF curve fits, 2 sets of distances were computed. One set consisted of 15 distances from the centroid to the dentition of each of MX and MD arch. In addition to these 15 distances, their x- and y-components were also calculated, yielding a set of 45 variables for subsequent analysis (Fig 4). The justification for including the x- and y-components is that a major change in shape might be in the direction of a

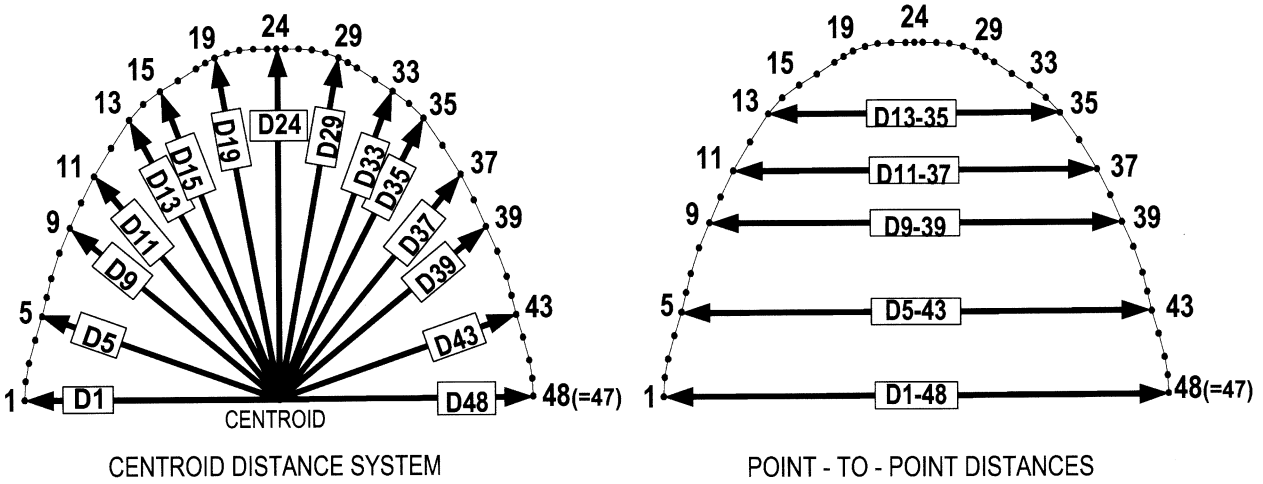

Fig 4. Fifteen centroid-based and 5 individual distances. These are *D1*, left distobuccal cusp, second molar; *D5*, left distobuccal cusp, first molar; *D9*, left second premolar; *D11*, left first premolar; *D13*, left canine tip; *D15*, left distal aspect, lateral incisor; *D19*, left distal aspect, central incisor; *D24*, midpoint between central incisors; *D29*, right distal aspect, central incisor; *D33*, right distal aspect, lateral incisor; *D35*, right canine tip; *D37*, right first premolar; *D39*, right second premolar; *D43*, right distobuccal cusp, first molar; *D48*, right distobuccal cusp, second molar. *D1-48*, *D5-43*, *D9-39*, *D11-37*, and *D13-35* are individual distances to above points. These 15 centroid-based distances and 5 individual distances represent 20 variables used to describe dental arch. Points are double original numbers (Fig 1) because EFF curve was constructed with 2× number of data points to ensure smoother fit.

component and not along the distance itself. The second set of distances was composed of the 5 point-to-point distances.

Before applying a 2-way multivariate analysis of variance (MANOVA) to test the above 2 contrasts (sex and type), a correlation matrix was computed (all statistical tests were run with Statistica 5.1; Statsoft, Tulsa, Okla). The purpose of this step was 2-fold: (1) to remove variables that displayed high correlations, because such variables do not add much information, and (2) to reduce the rather large number of variables (50 centroid-based and point-to-point distances). This was carried out by examining the pairwise correlations and removing 1 variable of each pair that displayed values equal to or greater than 0.80. Of the original 50 variables, 27 were retained for further analysis.

A second statistical approach involved the application of stepwise discriminant functions[24] to assess the group structure, test for the percentage of misclassifications, and provide a visual display of the variability in the dental arches. Because many variables were involved (27 distances), this requires the use of multivariate statistical procedures, such as discriminant functions.

Most discriminant function programs generate a variety of computations, such as an estimate of how close the members of a group are to each other and to members of other groups. This information is available from a "classification" matrix, which calculates the percentage of correctly identified members of a group (Table I). The "distance" of each member from another member is calculated from the Mahalanobis D^2 statistic (Table II). Finally, it is useful to be able to display these "distances" between members. These 27 remaining distances have been "collapsed" into a new set of uncorrelated variables (called canonical variates) and displayed as a 2-dimensional graph (Figs 7 and 8).

RESULTS

Computer-generated plots of the MX and MD arch outlines based on sex are shown in Figure 5. The means (female versus male) for group I (controls) are on the left, and those for group II (crowded dentitions) are on the right. The plots have been standardized for size and superimposed on the centroid. In the case of controls, female subjects display a longer and narrower dental arch than males. This pattern is similar for both arches. In contrast, for group II, not only is this difference much less apparent but also the patterns of the MX and MD arches are distinctly different.

A 2-way MANOVA was separately computed for the size-standardized (shape only) MX and MD data

Table I. Classification matrices derived from discriminant function analysis

	% correct	Control females	Control males	Crowding females	Crowding males
MX distances					
Control females	59.18	29	19	1	0
Control males	76.81	16	53	0	0
Crowding females	83.33	4	2	50	4
Crowding males	57.14	0	0	6	8
Total	72.91	49	74	57	12
MD distances					
Control females	55.10	27	22	0	0
Control males	84.06	9	58	2	0
Crowding females	66.67	3	10	42	8
Crowding males	35.71	0	2	7	5
Total	67.69	36	92	51	13

Maxillary (MX) and mandibular (MD) data are shown. Data has been standardized for size, so only shape differences are involved. Although good separation is maintained between control and crowding cases, misclassifications are present between females and males within each group.

Table II. Discriminant results for size-standardized MX and MD data

	Control females	Control males	Crowding females	Crowding males
MX distances				
Control females		1.44	10.72	15.39
Control males	2.34**		13.38	16.75
Crowding females	16.31***	24.31***		4.32
Crowding males	9.05***	10.51***	2.64***	
MD distances				
Control females		1.24	7.10	10.51
Control males	2.01*		6.62	9.91
Crowding females	11.06***	12.36***		4.11
Crowding males	6.19***	5.72***	2.54**	

For MX data (top half of table) and MD data (bottom half), values above diagonal refer to actual Mahalanobis D^2 distances and values below diagonal are the F values. Statistically significant D^2 distances are present between groups.
*$P < .05$; **$P < .01$; ***$P < .001$.

sets with the 2 "between effects," type (control versus crowding) and sex (male versus female). For the MX data, both type and sex were statistically significant ($P < .001$ level; type: Wilks' $\lambda = 0.358$; sex: Wilks' $\lambda = 0.810$). The interaction term (type $\times$ sex) was statistically insignificant. Univariate F tests for the MX "type" contrast displayed statistical significance for 10 of 14 retained distance variables: D5, D11, D13, D15, D19, D33, D35, D37, D43, and D11-D37. For the "sex" contrast, only 5 of the 14 retained distance variables showed statistical significance: D1, D33, D37, D43, and D11-D37.

For the MD data, only the type contrast was statistically significant ($P < .001$ level; type: Wilks' $\lambda = 0.593$). The interaction term (type $\times$ sex) was statistically insignificant. Univariate F tests for the MD "type" contrast displayed statistical significance for 7 of 13 retained distance variables: D11, D13, D24, D35, D37, D9-D39, and D11-D37.

Computer-generated plots of the MX and MD arch outlines based on type are shown in Figure 6. On the left are the means (control versus crowding) for the females and on the right the means for the males. These plots have also been superimposed on the centroid and standardized for size. Not surprisingly, clear differences are evident here. The pattern is particularly apparent for the MX comparisons and less so for the MD comparison.

The next issue addressed was to see the variation in the control and crowding cases. For this purpose, stepwise discriminant functions were chosen. Table I shows the classification matrix of the size-standardized MX data. Although reasonably good separation is maintained between the control and the crowding cases, some misclassifications, especially between sexes within each group, are present. Table I also shows the classification matrix for the MD data.

Figures 7 and 8 show plots of the first and second

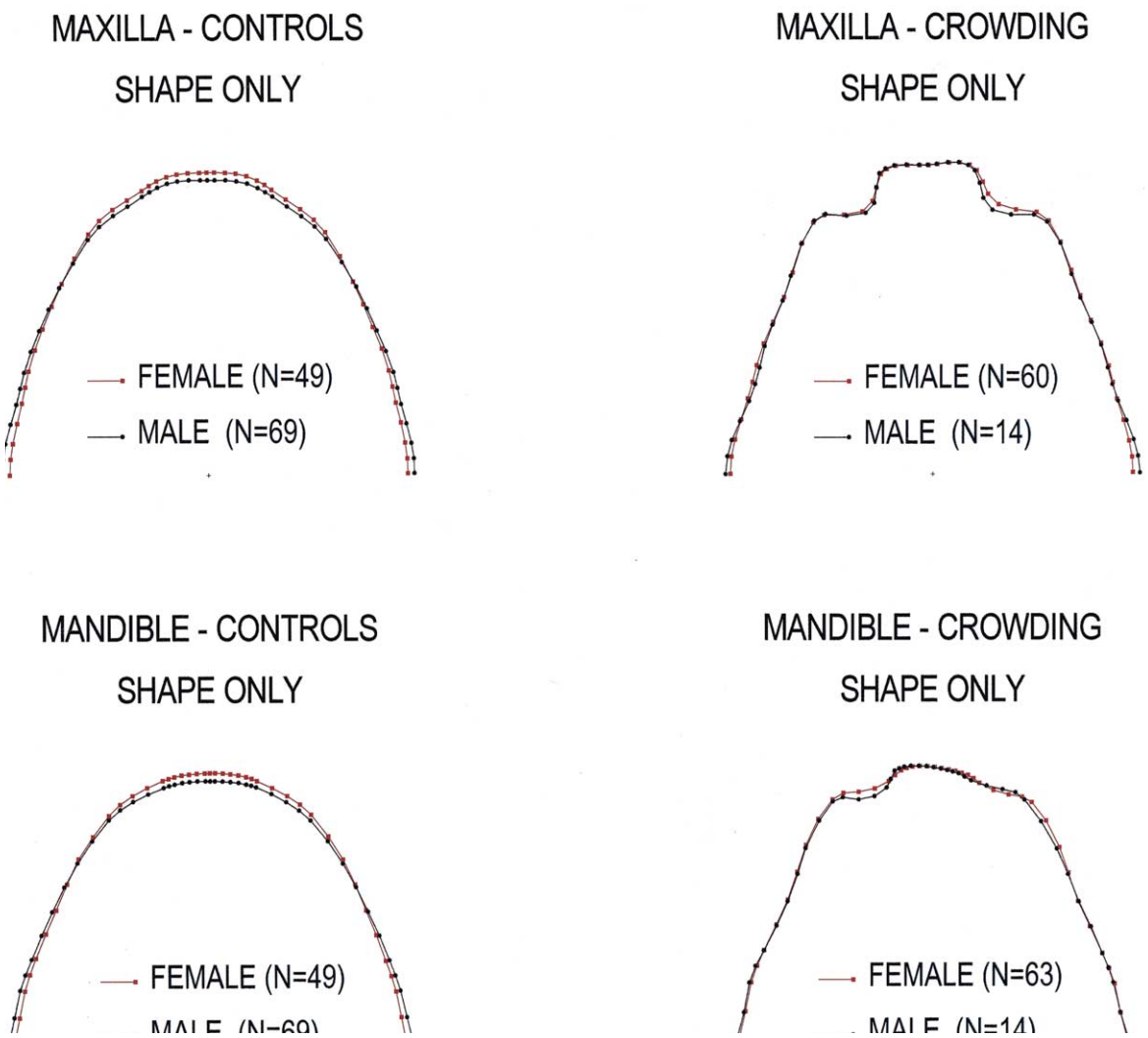

Fig 5. Computer-generated plots of mean MX and MD arch outlines. Two plots on left are superimpositions of mean females on males for controls; on right are superimpositions of mean females on males for crowding cases. Data have been standardized for size, so only shape differences are involved. Plots have been centroid-superimposed on line connecting distobuccal second molar cusps.

canonical axes for the size-standardized MX and MD data, respectively, derived from the discriminant analysis. Table II shows the actual Mahalanobis D^2 values for the MX and MD data shown in Figures 7 and 8. The statistically significant D^2 values in Table II are above the respective diagonals (MX above, MD below), and their *F* values are below the diagonals.

DISCUSSION

The results demonstrate that EFFs satisfactorily fit not only the dental arch of the controls but also the arch of the crowding cases, readily facilitating comparison between these groups. Moreover, the ability to standardize for size with the bounded area allows for an assessment of shape, which is minimally influenced by size considerations. This became important for determining the presence of sexual dimorphism in dental arch shape, in contrast to size. Sexual dimorphism with respect to size is generally obvious and present in the dental arches, with few exceptions. However, shape differences due to sex might be subtle and not so easily detected. The data here, especially for the controls, exhibited an unexpected pattern, in that definite shape differences between females and males emerged. Females, on average, had a longer anteroposterior length and a narrower width in the molar region than males

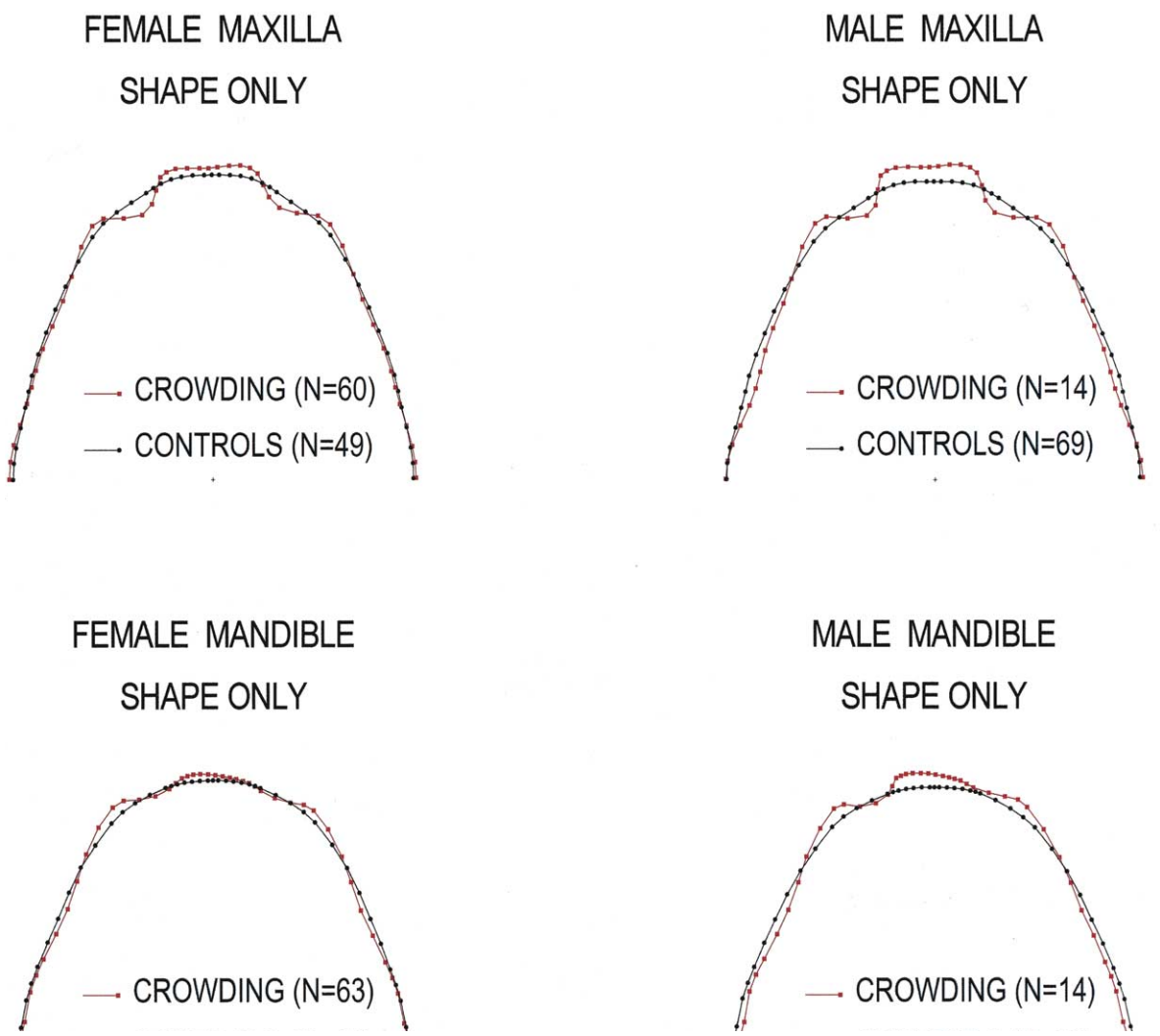

Fig 6. Computer-generated plots of mean MX and MD arch outlines. Two plots on left are superimpositions of controls on crowding cases for females; on right are superimpositions of controls on crowding cases for males. Data have been standardized for size, so only shape differences are involved. Mean plots have been superimposed on centroid and line connecting distobuccal second molar cusps.

(Fig 5). This pattern was present in both arches. Although the same pattern undoubtedly is also present in the crowding cases, it was not expressed as clearly because of the confounding effect of crowding.

In the crowding cases, the mean plots show surprising similarities between males and females. This pattern suggests that crowding is not purely random but strongly constrained. The pattern, moreover, is distinctly different between the arches, with asymmetry now present. Reasons for this difference between the MX and MD dentitions are not readily obvious but presumably might be due to differences in mastication between the MX and MD jaws with the somewhat compromised anterior dentition.

The discriminant function analysis showed that the crowding cases exhibited considerably more variability than did the controls. Given this large variability in the crowding cases, cluster analysis is being contemplated in a future study to determine whether there are subgroups in the crowding cases.

CONCLUSIONS

This study has demonstrated the usefulness of EFFs for numerically describing the shape of structures in the

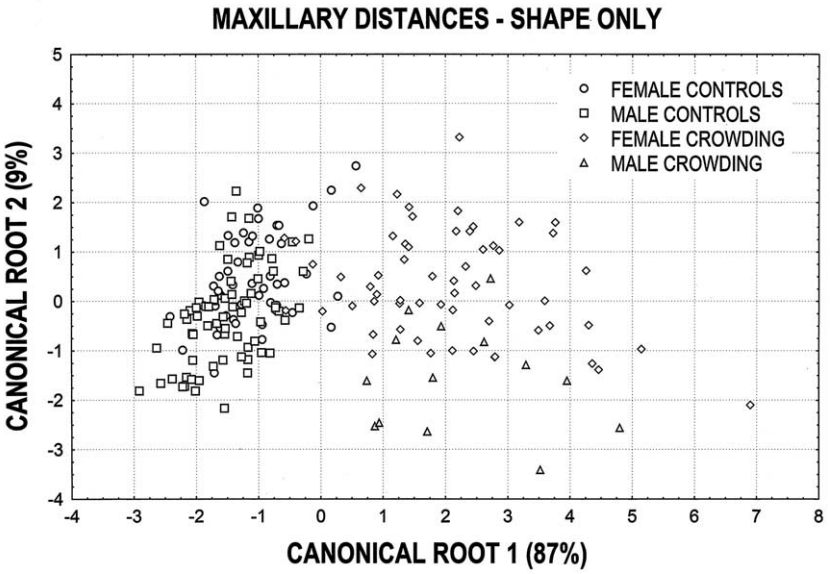

Fig 7. Plot of canonical axes 1 versus 2 derived from discriminant function analysis. Maxillary control and crowding groups are broken down by sex. Data have been standardized for size, so only shape differences are involved.

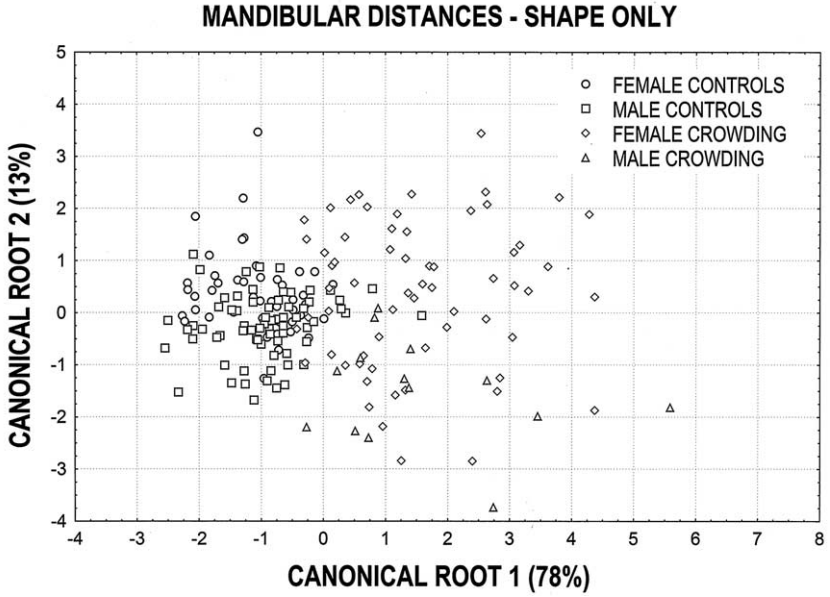

Fig 8. Plot of canonical axes 1 versus 2 derived from discriminant function analysis. Mandibular control and crowding groups are broken down by sex. Data have been standardized for size, so only shape differences are involved.

craniofacial complex, specifically the MX and MD arches. The use of EFFs has clearly displayed the differences between sexes as well as an asymmetrical pattern of crowding in the dental arches. Both aspects only became recognizable as a function of the application of EFFs. With the use of such procedures as EFFs, it might become feasible to develop standards of dental arch shape. Such clinical standards might prove useful for orthodontic, prosthodontic, and oral surgery treatment planning.

We thank Dr Steve Ahn, formerly of the Section of Orthodontics, University of California-Los Angeles School of Dentistry, for his assistance with analysis of the dental cast data and Dr Kazutaka Kasai, Chair, Department of Orthodontics, Nihon University School of Dentistry at Matsudo, for his support.

REFERENCES

1. Inoue N. Tooth to denture discrepancy in human evolution. J Anthrop Soc Nippon 1980;88:69-82.
2. Kasai K, Kawamura A, Kanazawa E. A comparative study of dental arch and horizontal section of the mandible in Jomon and modern Japanese using CT scanning. Orthod Waves 1999;58: 193-8.
3. Beecher RM, Corruccini RS. Effects of dietary consistency on craniofacial and occlusal development in the rat. Angle Orthod 1981;51:61-9.
4. Varrela J. Dimensional variation of craniofacial structures in relation to changing masticatory functional demands. Eur J Orthod 1992;14:31-6.
5. Rudge SJ. Dental arch analysis: arch form. A review of the literature. Eur J Orthod 1981;3:279-84.
6. MacConail MA, Scher EA. The ideal form of the human dental arcade, with some prosthetic application. Dent Rec 1949;69:285-302.
7. Pepe SH. Polynomial and catenary curve fits to human dental arches. J Dent Res 1975;54:1124-32.
8. Biggerstaff RH. Three variations in dental arch form estimated by a quadratic equation. J Dent Res 1972;51:1509.
9. Sampson PD. Dental arch shape: a statistical analysis using conic sections. Am J Orthod 1981;79:535-48.
10. Sampson PD. Statistical analysis of arch shape using conic sections. Biometrics 1983;39:411-23.
11. Jones ML, Richmond S. An assessment of the fit of a parabolic curve to pre- and post-treatment dental arches. Br J Orthod 1989;16:85-94.
12. BeGole EA. Application of the cubic spline function in the description of dental arch form. J Dent Res 1980;59:1549-56.
13. Lu KH. An orthogonal analysis of the form, symmetry and asymmetry of the dental arch. Arch Oral Biol 1966;11:1057-69.
14. Ferrario VF, Sforza C, Miani A Jr, Tartaglia G. Mathematical definition of the shape of dental arches in human permanent healthy dentitions. Eur J Orthod 1994;16:287-94.
15. Kuhl FP, Giardina CR. Elliptic Fourier features of a closed contour. Comput Graphics Image Processing 1982;18:236-58.
16. Rohlf FJ, Archie JW. A comparison of Fourier methods for the description of wing shape in mosquitos (Diptera: culicidae). Syst Zool 1984;33:302-17.
17. Ferson S, Rohlf FJ, Koehn RK. Measuring shape variation of two-dimensional outlines. Syst Zool 1985;43:59-68.
18. Lestrel PE. Some approaches toward the mathematical modeling of the craniofacial complex. J Cranofac Genet Dev Biol 1989;9:77-91.
19. Lestrel PE. A new method for analyzing complex two-dimensional forms: elliptical Fourier functions. Am J Hum Biol 1989;1:149-64.
20. Lestrel PE, Kerr JWS. Quantification of functional regulator therapy using elliptical Fourier functions. Eur J Orthod 1993;15: 481-91.
21. Lestrel PE. Fourier descriptors and their applications in biology. Cambridge, United Kingdom: Cambridge University Press; 1997.
22. Lestrel PE. Morphometrics for the life sciences. Singapore: World Scientific; 2000.
23. Ursi WJ, Trotman CA, McNamara JA Jr, Behrents RG. Sexual dimorphism in normal craniofacial growth. Angle Orthod 1993; 63:47-56.
24. Davis JC. Statistics and data analysis in geology. 2nd ed. New York: John Wiley & Sons; 1986.